Macromolecules

ARTICLE

pubs.acs.org/Macromolecules

# Orienting Semiconducting Nanocrystals on Nanostructured Polycarbonate Substrates: Impact of Substrate Temperature on Polymorphism and In-Plane Orientation

Christelle Vergnat, Virginie Landais, Jean-François Legrand, and Martin Brinkmann*

Institut Charles Sadron, CNRS-Université de Strasbourg, 23 rue du loess, 67034 Strasbourg, France

Supporting Information

**ABSTRACT:** This paper reports a systematic investigation of the growth mechanism of zinc phthalocyanine, a p-type semiconductor, on oriented polymer substrates of bisphenol A polycarbonate (PC). It focuses on the impact of the substrate temperature on the polymorphism and the in-plane orientation of the ZnPc nanocrystals. The study combines transmission electron microscopy, X-ray diffraction, atomic force microscopy, UV−vis absorption spectroscopy, and force field-based molecular calculations. Large areas of oriented PC substrates are prepared by a simple process that combines mechanical rubbing and solvent-induced crystallization. The PC substrates show a smooth semicrystalline morphology with a preferential $(a,c)$ surface of crystalline lamellae with a high in-plane orientation of the polymer chains. These substrates induce a unidirectional orientation of ZnPc nanocrystals with a preferred contact plane. The selection of the preferred ZnPc in-plane growth direction relies on a "self-amplified" mechanism whereby a fraction of ZnPc nanocrystals oriented by the polycarbonate substrate enforces the orientation of neighbouring domains during film growth. Regarding polymorphism, two domains of substrate temperature ($T_s$) are evidenced. For 33 °C ≤ $T_s$ ≤ 115 °C, ZnPc nanocrystals grow exclusively in the α form. The determined crystal structure of α-ZnPc ($a$ = 1.23 nm, $b$ = 0.38 nm, $c$ = 1.28 nm and $\gamma = 96 \pm 1°$, $Z = 1$) is isomorphous to the recently refined structures of CuPc and CoPc. For 115°C ≤ $T_s$ ≤ 200°C, ZnPc films consist of both α and $\beta$ nanocrystals with a gradual increase of the proportion of $\beta$-form with increasing $T_s$. The onset of the beta polymorph growth coincides with a marked change in the nanocrystal size. The $\beta$ phase appears when the ZnPc nanocrystals reach some critical dimensions which can be estimated from the $T_s$-dependence of the nanocrystal size. The relative stability of the α and $\beta$ polymorphs is explained by the balance of the bulk and the surface energy of the nanocrystals. A simple model is developed to predict and force-field based molecular simulations are used to estimate the critical dimensions of the ZnPc nanocrystals.

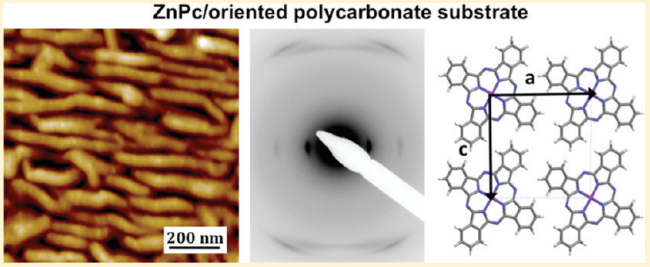


## I. INTRODUCTION

Controlling the growth and self-assembly of small molecules on surfaces in order to generate and organize nanostructured objects and patterns is a challenging research field tackled in a many different ways.[1−6] One possible approach makes use of epitaxial growth of small molecules deposited from the vapor phase on orienting substrates.[7−9] The control of the preferential orientation of the $\pi$-stacking direction in a thin film, i.e. the direction of favorable charge transport in conjugated materials, is essential in order to improve the transport performances in devices such as organic field effect transistors (OFETs) and organic solar cells.[10] Among the numerous organic semiconductors, metallophthalocyanines have attracted much interest because of their high thermal and chemical stability, combined with unique electronic properties.[11] Zinc phthalocyanine (ZnPc) has emerged as a key material in the elaboration of organic solar cells, especially when associated with $C_{60}$ fullerene in bulk heterojunctions or in bilayer devices.[12−15] It is therefore highly desirable to understand and master the inherent polymorphism and growth mechanism of ZnPc on various substrates including polymer substrates that are necessary to fabricate devices on flexible substrates. In order to integrate these materials in viable and efficient devices, it is necessary to establish the relationships between the processing conditions (deposition rate, substrate temperature, film thickness), the structure and morphology of the films, and the corresponding transport properties.[16] This implies to understand the emergence of polymorphism in the films of these macrocyclic $\pi$-conjugated materials since it impacts directly the device performances.[17] It is now well-known that phthalocyanines containing a divalent first-transition metal exhibit different polymorphic forms, especially the α and $\beta$ forms.[18−21] However, the polymorphism of ZnPc is peculiar in that three different α modifications exist, as identified by high resolution transmission electron microscopy (HR-TEM) in evaporated thin films.[18] Although the polymorphism of metallophthalocyanines has been

**Received:** February 15, 2011
**Revised:** April 13, 2011
**Published:** May 02, 2011

ACS Publications © 2011 American Chemical Society

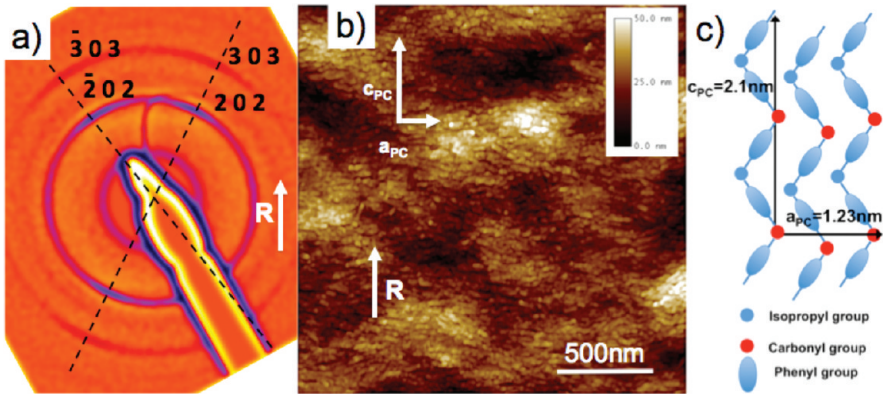


**Figure 1.** (a) ED pattern of an oriented PC substrate after solvent induced crystallization (2 h) in acetone. (b) Lamellar morphology of the oriented PC films observed by AFM after 6 min exposure to acetone vapors. The rubbing direction is marked by an arrow (*R*). (c) Schematic illustration of the molecular structure of PC chains in the crystalline unit cell as determined by Bonart.[35] For clarity, only top-surface polymer chains are represented.

extensively investigated in the eighties and nineties, recent studies have demonstrated that the α form of CuPc and CoPc is not correctly described by the crystal structure of α-PtPc.[22−24] It is therefore important to investigate carefully the exact crystalline forms of ZnPc present in evaporated thin films.

The α→$\beta$ phase transformation is achieved in thin films by thermal annealing, by solvent vapor annealing, or by controlling the substrate temperature during deposition.[25−28] This phase transformation has been explained in terms of size effects by Iwatsu using lattice energy calculations.[29] Below and above some critical dimensions, the phthalocyanine nanocrystals grow preferentially in the α structure and in the stable $\beta$ form, respectively. The impact of crystal size on the preferential polymorph formed in thin films seems to be a general phenomenon, also observed in the case of pentacene for instance.[30] There has been no experimental determination of this critical size in the case of phthalocyanines.

To address these various points, we have taken advantage of the highly oriented and well-defined morphology of phthalocyanine nanocrystals deposited on an oriented polymeric substrate of bisphenol A polycarbonate. Oriented and nanostructured substrates of polycarbonate (PC) are readily fabricated by (i) rubbing an amorphous PC film and (ii) initiating the growth of oriented PC lamellae by solvent induced crystallization.[31,32] The PC alignment layers show a periodic and regular nanostructured surface, a high level of order at the length scale of polymer chains and a reduced surface roughness. PC layers induce alignment of molecular materials including acenes, phthalocyanines, coronene, bisazo dyes and generate ordered arrays of gold nanoparticles. Highly oriented nanocrystals of CuPc with a narrow size distribution can be grown on the PC substrate, which is of interest for performing a statistical analysis of the nanocrystal domain size versus deposition conditions.[33,34]

The present work is organized as follows: (i) determination of the surface structure of the PC substrate, (ii) emergence of in-plane orientation with increasing film thickness, (iii) impact of substrate temperature on nanocrystal morphology and orientation, (iv) $T_s$-dependence of polymorphism with special attention given to the crystal structure of the α polymorph, and (v) determination of the critical nanocrystal dimensions of ZnPc for the α → $\beta$ phase transformation.

## II. EXPERIMENTAL SECTION

The preparation procedure for the PC alignment layers is described in detail in references[31] and.[32] ZnPc thin films were grown on the PC substrates by sublimation in high vacuum using an Edwards Auto306 evaporator system. The ZnPc starting material (Aldrich) was purified by sublimation from a quartz crucible under high vacuum ($10^{-5}$ mbar) and recovered in a second crucible used afterward for the deposition of the films. The base pressure of the evaporation chamber was $10^{-6}$ mbar. Films were deposited at a constant deposition rate $\tau$ = 2.0 nm/min controlled by using a quartz microbalance placed in the vicinity of the substrate holder. To prevent structural modifications of the films by annealing after deposition, the temperature of the sample holder was rapidly cooled to room temperature (cooling rate: 0.5−1.0 °C/s) by using a liquid nitrogen cooling system.

The PC substrate orientation was first investigated by polarized optical microscopy using a LEICA DM-RX microscope. The surface topography of the polymer alignment layers and the phthalocyanine films was investigated by tapping mode AFM (Nanoscope III) using $Si_3N_4$ cantilevers oscillating at a frequency in the range 250−300 kHz. Vizualisation of the polymer film topography was performed under soft tapping conditions (drive amplitude variation below 15% with respect to the free cantilever). The structure and morphology of evaporated phthalocyanine films of thickness 50 nm were investigated by transmission electron microscopy (TEM) in the bright field mode (BF) and by electron diffraction (ED) with a 120 kV Philips CM12 electron microscope equipped with a MVIII CCD camera (Soft Imaging Systems). To this aim, the phthalocyanine/substrate samples were coated with an amorphous carbon film, floated off on a diluted aqueous HF solution (5%) and transferred onto copper microscope grids. For the HR-TEM imaging, a TECNAI $G^2$ 200 kV microscope equipped with a FEI Eagle 2K CCD camera was used. Image treatments e.g. fast Fourier transforms (FFT) and statistical anaysis of the nanocrystal size distribution were performed by using AnalySIS (Soft Imaging System) software. A high-pass filter was used to enhance the diffraction peaks in the electron diffraction patterns of Figure 7. The statistics of the island size distribution was performed on a set of 200−300 nanocrystals. X-ray diffraction in ($\theta$, 2$\theta$) configuration was performed on a Siemens D500 diffractometer. A calibration with NaCl crystals was performed in order to measure accurately the position of the ZnPc diffraction peaks at low angles (5−10°). For the calibration with NaCl, a first scan was performed in the range 5−60° with an angular step of 0.02° and a counting time of 60 s per step. A second scan was performed in the range 5−10° with an angular step of 0.01° and a counting time of 60 s per step. The optical anisotropy of the oriented phthalocyanine films was investigated by UV−vis−near IR absorption (300−900 nm) spectroscopy using a Shimadzu UV-2101PC spectrometer with polarized incident light and a spectral resolution of 1 nm. The film orientation with respect to the incident light was controlled by means of a

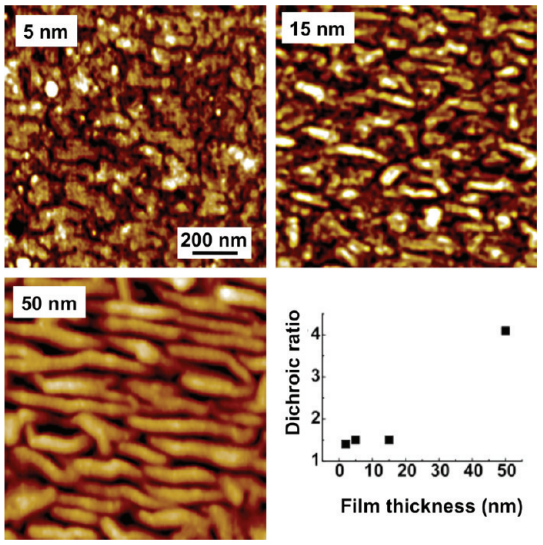


**Figure 2.** Evolution of the film topography probed by AFM for ZnPc films deposited on oriented and nanostructured PC substrates as a function of increasing film thickness for a constant substrate temperature of 100 °C. The plot shows the variation of the dichroic ratio (measured at 630 nm) as a function of film thickness.

goniometer: the ∥ orientation is defined such that the incident beam polarization is parallel to the PC rubbing direction ($c_{PC}$ axis).

## III. RESULTS AND DISCUSSION

**a. Structure of the PC Substrate.** Highly oriented and nanostructured polymer layers of bisphenol A polycarbonate (PC) can be prepared by combining the mechanical rubbing of the films with solvent induced crystallization in acetone vapor.[31] The crystallization of the rubbed PC films proceeds from the free polymer surface down into the bulk of the films as the exposure time of the films to the solvent vapor increases. The PC films obtained for 2 min exposure to acetone vapors exhibit only a very thin oriented and crystallized surface layer which does not diffract sufficiently the electrons in a TEM.[31,32] Accordingly, a thick oriented and crystalline PC layer suitable for electron diffraction analysis was grown by exposing the rubbed films for 2 h to acetone vapors. Figure 1 depicts the corresponding ED pattern along with the surface topography probed by AFM. Overall, the ED pattern is similar to that obtained by Bonart on mechanically drawn PC films.[35] It shows two intense arced reflections at ±30° from the rubbing direction with reticular distances of 0.52 and 0.344 nm. On the basis of the unit cell parameters reported by Bonart for bisphenol A polycarbonate, these reflections are indexed as 2 0 2 and 3 0 3 respectively. The structure of PC proposed by Bonart involves four chains per unit cell with a characteristic zigzag conformation of the PC chain and unit cell parameters: $a$ = 1.23 nm, $b$ = 1.01 nm, $c$ = 2.08 nm, $\alpha = \gamma = 90°$, and $\beta = 84°$. The 2 0 2 and the 2 0 −2 reticular planes contain the two chain segments of the zigzag as illustrated in Figure 1c. Accordingly, the observation of $h$ 0 $L$ reflections suggests that the oriented and crystallized PC substrates consist of PC lamellae with a (0 1 0) surface. Additional experimental evidence obtained by grazing incidence X-ray diffraction confirm this preferential orientation of PC crystals in the oriented substrates.[36]

The ED pattern in Figure 1 also indicates a rather large distribution of the in-plane orientation of the crystalline PC lamellae. From the azimuthal line profile (not shown), the measured half width at half-maximum of the 2 0 2 peak intensity is typically 10°. This value is consistent with the fluctuations of the in-plane orientation of the lamellae observed in the AFM image which is already visible after 6 min exposure of the rubbed PC films to acetone vapors (Figure 1.b). It is also consistent with the observed misalignment of polyimide chains observed in rubbed thin films by Toney et al.[37]

**b. Emergence of In-Plane Orientation with Increasing Film Thickness.** In order to have a better understanding of the orientation mechanism at play on PC substrates, ZnPc films of increasing thickness in the range 1 nm -50 nm were deposited at a constant substrate temperature ($T_s$ = 100 °C) and deposition rate ($\tau$ = 2 nm/min). Parts a−c of Figure 2 depict the evolution of film morphology (AFM topography) with increasing film thickness $t$ with concommittent evolution of the dichroic ratio measured at $\lambda$ = 630 nm with increasing film thickness (Figure 2d).

For $t$ = 5 nm, the ZnPc films show a granular morphology of nanodomains with ill-defined contours. The dichroic ratio is close to 1, indicating poor in-plane orientation of the ZnPc domains. In films of 15 nm thickness, elongated nanocrystals are apparent. When $t$ = 50 nm, the films consist exclusively of oriented and tightly packed nanocrystals with well-defined grain boundaries, also attested by the much higher dichroic ratio of 4.5. This first sequence of AFM images suggest that elongated nanocrystals may be formed by coalescence of smaller subdomains. Figure 3 shows a HR-TEM image for a ZnPc film of 50 nm grown at $T_s$ = 100 °C. Crystalline nanodomains with well-defined molecular stacks are clearly observed with an interstack period of 1.23 nm. Some fluctuations of the in-plane orientation is observed as indicated by the FFT shown as an inset in Figure 3. More interestingly, the apparent length of the nanocrystals seen by AFM, i.e., 250 nm does not coincide with the average length of the columnar stacks seen by HR-TEM. From the HR-TEM images, the crystalline domains show a coherent orientation of the molecular stacks over a maximal distance of 50 nm, i.e., much below the apparent nanocrystal length measured by AFM. This result supports a growth mechanism whereby larger oriented nanocrystals are formed by coalescence of smaller nanocrystalline domains that can partially reorient during the growth process. A similar situation has been reported for the growth of pentacene and titanyl phthalocyanine (PcTiO) on oriented poly(tetrafluoroethylene) substrates[38,39] and α-sexiphenyl on mica substrates.[40]

**c. Impact of Substrate Temperature on Nanocrystal Morphology and Orientation.** Figure 4 depicts the evolution of the ZnPc film morphology probed by AFM substrate as a function of the temperature $T_s$. A statistical analysis of the domain size was performed to quantify the morphological modifications of the ZnPc domains with increasing $T_s$. The statistics was performed over 200−300 domains and helped determine the average width and length of the ZnPc nanocrystals and the corresponding aspect ratio (length/width). Figure 5 depicts the $T_s$-dependence of the average width and length of ZnPc nanocrystals as observed by AFM. The morphological changes of the ZnPc domains concern their average shape, size and in-plane orientation.

Regarding the shape of the ZnPc domains, a progressive transition from a hemispherical shape for $T_s$ = 33 °C toward elongated needles for $T_s$ = 60 °C is observed. As a consequence,

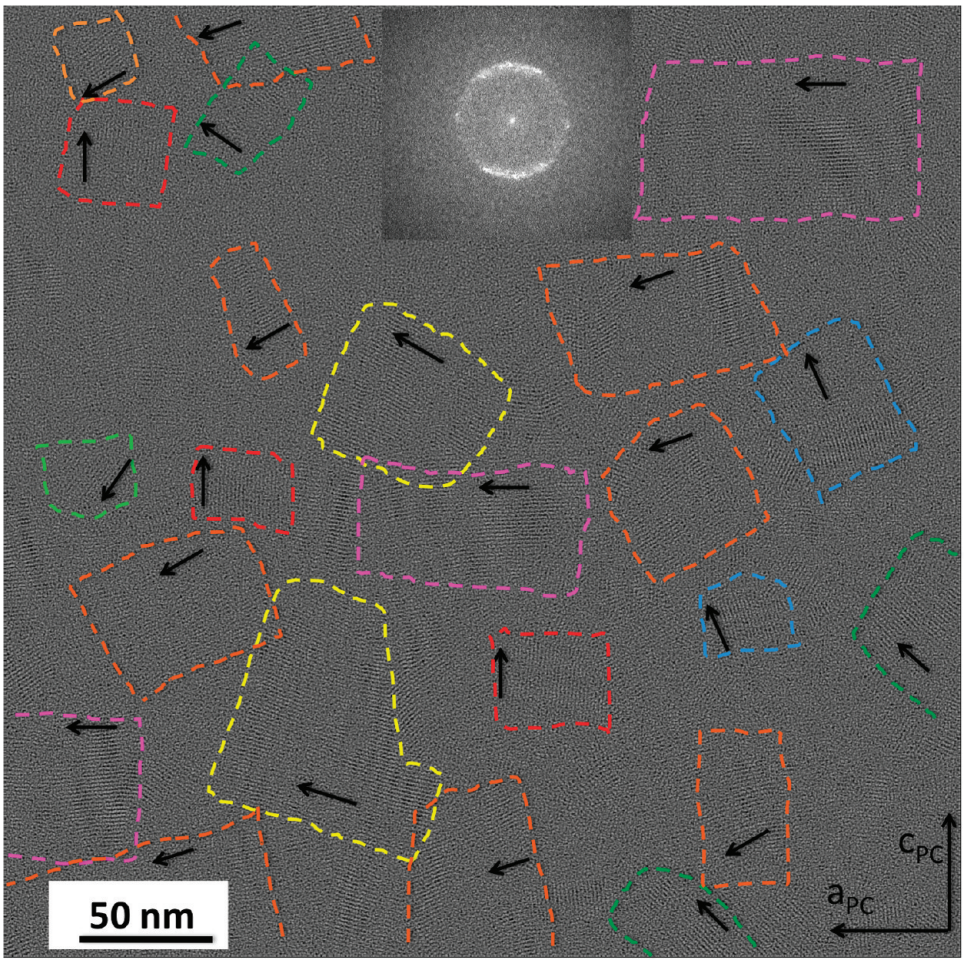


**Figure 3.** HR-TEM image of an oriented ZnPc thin films grown at $T_s$ = 100 °C (50 nm). Crystalline domains are observed along different in-plane directions highlighted by arrows. Estimated contours of nanocrystalline domains have been drawn as dotted lines. The fast Fourier transform has also been included in the figure showing essentially two intense arcs corresponding to the 1.23 nm intercolumn period of α ZnPc.

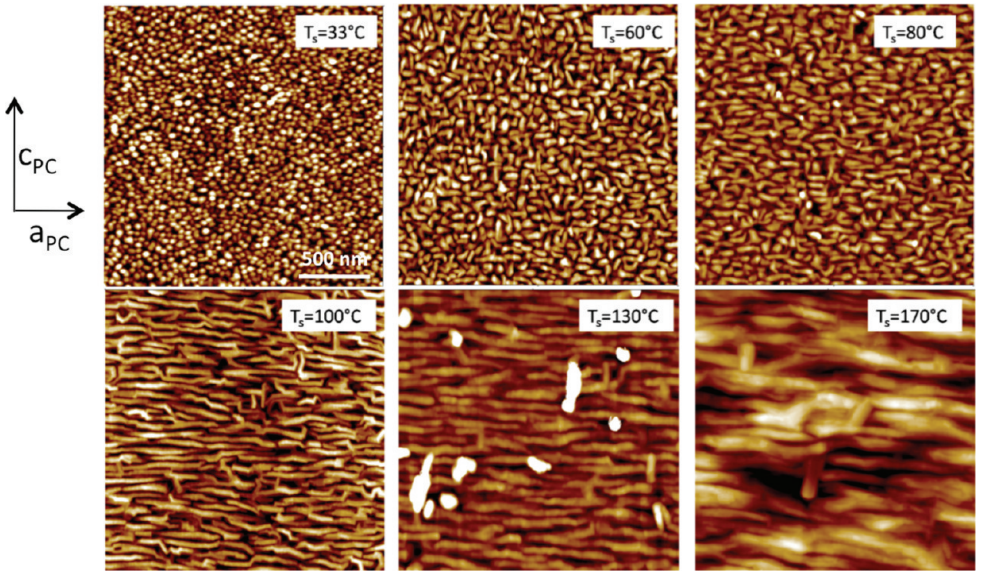


**Figure 4.** Evolution of the thin film morphology with increasing substrate temperature for ZnPc thin films (50 nm) deposited on oriented and nanostructured PC substrates. For all the images, the PC chain direction is oriented vertically.

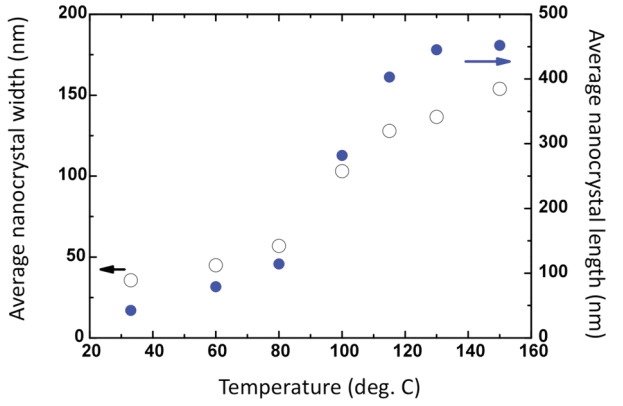


**Figure 5.** Evolution of the statistical length and width of the ZnPc nanocrystals grown on oriented and nanostructured PC substrates as a function of substrate temperature.

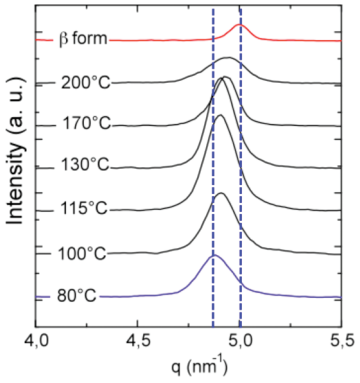


**Figure 6.** Out-of-plane X-ray diffraction patterns for ZnPc thin films (50 nm) on oriented PC substrates as a function of increasing substrate temperature $T_s$. The pure $\beta$ form ZnPc film was obtained by solvent vapor annealing (see text).

the aspect ratio of the crystals tends to increase smoothly between 1 and 1.9 in the range 33 °C ≤ $T_s$ ≤ 80 °C. Between 80 and 130 °C, the nanocrystal's shape shows a pronounced evolution with a marked increase of the aspect ratio to a value of 3−3.5 for $T_s$ = 130 °C. Incidentaly, the growth of elongated nanocrystals coincides with the emergence of preferred in-plane orientation as evidenced by UV−vis absorption spectroscopy and electron diffraction (vide infra).

Concerning the evolution of the nanocrystal size, the same trend is observed as for their shape (see Figures 4 and 5): (i) a smooth and progressive increase of length and width until $T_s$ = 80 °C, (ii) a marked increase in the range 80 °C ≤ $T_s$ ≤ 130 °C and (iii) an apparent saturation of the nanocrystal's length and width for 130 °C ≤ $T_s$ ≤ 160 °C. However, it is worth to stress that the estimation of the nanocrystal's length is made difficult as the grain boundaries in that direction are difficult to evidence by AFM (especially for $T_s$ ≥ 150 °C). As shown hereafter, the abrupt increase of the nanocrystal dimensions around $T_s$ = 100 °C coincides with the growth of the $\beta$ form in the films.

Finally, the AFM topographic images also suggest a marked evolution of the in-plane orientation of the ZnPc domains. For $T_s$ = 33 °C, no clear in-plane orientation can be inferred because of the hemispherical shape of the ZnPc domains. For $T_s$ = 60 °C,

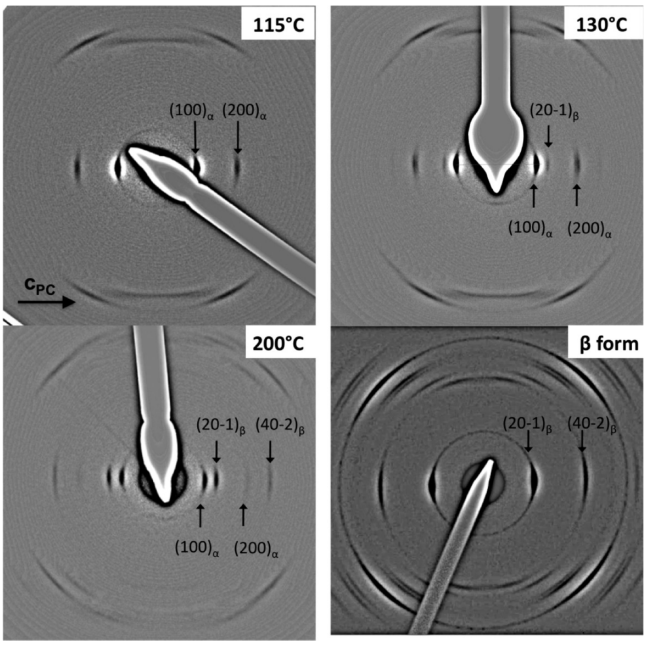


**Figure 7.** Evolution of the ED pattern of oriented ZnPc films on oriented PC substrates for $T_s$ in the range 115−200 °C. The equatorial reflections characteristic of the α and $\beta$ forms have been indexed and labeled.

two dominant populations of elongated ZnPc nanocrystals are observed ; they are oriented mainly parallel and perpendicular to the crystalline lamellae of the PC substrate. Electron diffraction shows that these nanocrystals have their stacking axis ($b$ axis) oriented parallel and perpendicular to the crystalline lamellae of the PC substrate. For $T_s$ ≥ 80 °C, the population parallel becomes dominant, suggesting that the selection of the in-plane orientation of ZnPc nanocrystals is determined by the substrate temperature.

**d. Dependence of Polymorphism on Substrate Temperature.** Phthalocyanine films are known to exhibit a characteristic polymorphism that depends on both the chemical nature of the substrate and the substrate temperature used during deposition. A first indication of the polymorphism of ZnPc on the PC substrates is obtained by X-ray diffraction in ($\theta$, $2\theta$) mode. Figure 6 depicts the evolution of the main diffraction peak in the specular configuration as a function of $T_s$

For $T_s$ = 33 °C, the main peak observed at $q$ = 4.88 nm$^{-1}$ corresponds to the interstack period of 1.28 nm (different from the in-plane period of 1.23 nm observed by ED). This peak increases in intensity and shifts to higher q values as $T_s$ increases up to 130 °C. For $T_s$ ≥ 130 °C, the peak's intensity decreases further, broadens and shifts to $q$ = 4.95 nm$^{-1}$. However, even for $T_s$ = 200 °C, the peak's position does not reach the value observed for pure $\beta$-ZnPc films i.e. $q$ = 5.0 nm$^{-1}$ ($d_{hkl}$ = 1.256 nm).[19] The large width of the main diffraction peak for $T_s$ = 200 °C is attributed to the overlap of the α and $\beta$ contributions, which are too close to be distinguished by X-ray diffraction measurements in the out-of-plane configuration. Accordingly, electron diffraction was used to obtain a clear-cut evidence for the polymorphic character of the ZnPc films.

Figure 7 shows the ED patterns of oriented ZnPc films (50 nm) grown on PC substrates for 115 °C ≤ $T_s$ ≤ 200 °C as well as a pure $\beta$-form film obtained after vapor treatment in

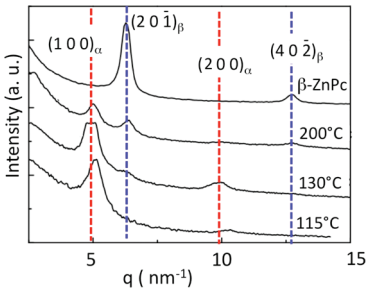


**Figure 8.** Cross section profile along the equator line of the ED patterns of oriented ZnPc films shown in Figure 7 showing the emergence of the characteristic peaks of the $\beta$-form. Note that the intensity of the $(1\,0\,0)_\alpha$ peak is saturated for $T_s$ = 130 °C.

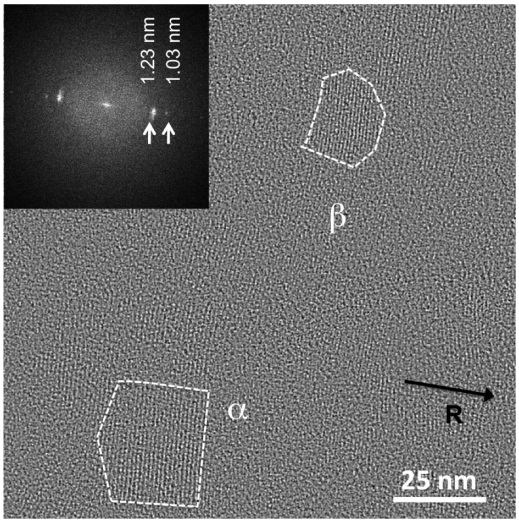


**Figure 9.** High-resolution TEM image of a 50 nm-thick ZnPc film grown at $T_s$ = 200 °C on an oriented substrate of PC and showing the coexistence of α and $\beta$ form nanocrystals. The inset shows the FFT of the HR-TEM image.

$CH_2Cl_2$ of a film deposited at 170 °C. Figure 8 shows the corresponding cross sectional profiles of the ED patterns along the equator line. On the equator of the ED pattern, the $\beta$-ZnPc film exhibits two well-defined reflections at 6.25 $nm^{-1}$ and 12.6 $nm^{-1}$ indexed as $(2\ 0\ -1)_\beta$ and $(4\ 0\ -2)_\beta$ respectively. The ZnPc films grown at $T_s$ = 115 °C show the characteristic $(1\,0\,0)_\alpha$ and $(2\,0\,0)_\alpha$ peaks of the α structure corresponding to $d_{hkl}$ = 1.20 ± 0.05 nm and 0.60 ± 0.03 nm, respectively. For $T_s$ = 130 and 200 °C, beside the characteristic peaks of the α structure, the peak at 6.25 $nm^{-1}$ (with the corresponding second order peak at 12.6 $nm^{-1}$) characteristic of the $\beta$ form is also present and tends to increase in intensity with increasing $T_s$. However, even for $T_s$ = 200 °C, the films are still polymorphic. Accordingly, the ED results demonstrate clearly the polymorphic nature of the ZnPc films grown on the PC substrate at $T_s \geq$ 130 °C. The coexistence of both α and $\beta$ nanocrystals is further evidenced by HR-TEM as seen in Figure 9 for a ZnPc film grown at $T_s$ = 200 °C. The HR-TEM image shows coexistence of crystalline domains with different stacking periodicities of 1.03 nm for the $\beta$ domains ($(2\ 0\ -1)_\beta$ planes) and 1.23 nm for the α domains ($(1\,0\,0)_\alpha$ planes).

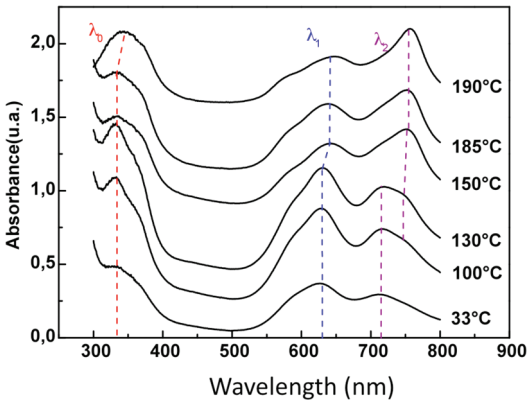


**Figure 10.** Evolution of the UV−vis absorption spectrum with increasing substrate temperature for oriented ZnPc thin films (50 nm) evaporated on oriented and nanostructured PC substrates.

UV−vis absorption spectroscopy confirms the polymorphic character of the films. Figure 10 depicts the evolution of the UV−vis absorption as a function of increasing $T_s$. All spectra show the characteristic Soret band centered at $\lambda_o$ in the range 335−350 nm and the structured *Q*-band ($\pi \rightarrow \pi^*$) with contributions at $\lambda_1$ and $\lambda_2$ (these two positions are characteristic signatures of the polymorph). For $T_s \leq$ 115 °C, the absorption spectra of the films in the *Q*-band region are dominated by two components located at $\lambda_1$ = 630 nm and $\lambda_2$ = 715 nm typical of the α form. For $T_s \geq$ 130 °C, a shoulder at 750 nm gradually increases in intensity and becomes a clear peak for $T_s$ = 200 °C. The first peak at $\lambda_1$ tends also to shift to 640 nm. Both these peaks at 640 and 715 nm are characteristic of the $\beta$ structure of ZnPc. Accordingly, both the ED and the UV−vis absorption results demonstrate the gradual increase of the $\beta$ phase content in the films when $T_s$ increases above 115 °C. However, even for $T_s$ = 200 °C, the ZnPc films are still polymorphic. The pure $\beta$-phase films are only obtained upon solvent vapor exposure.

**e. Identification of the α and *β* Polymorphs.** The α structure of various metallophthalocyanines like CuPc and CoPc in thin films and powders has long been considered isostructural to the structure of α-PtPc.[19] However, carefull investigations of the α structure of CuPc and CoPc revealed a molecular packing different from that determined for PtPc.[22−24] The crystal structure of α CuPc has been investigated by electron diffraction analysis yielding a simple triclinic unit cell with one molecule per cell, space group $P\bar{1}$ and $a$ = 1.289 nm, $b$ = 0.377 nm, $c$ = 1.21 nm and α = 96° ($\beta$ and $\gamma$ are almost equal to 90°).[24] Hoshino et al. have proposed two molecular packings (models I and II) which differ by the offset direction between two successive ZnPc molecules in a stack.[24] A structural model similar to model II of Hoshino was proposed for CoPc by Ballirano et al. using a Rietveld analysis of α powders.[22] The ED pattern of pure α-form ZnPc films grown at $T_s$ = 115 °C is shown in Figure 11.a. As illustrated in Figure 11.b, the overall ED pattern is the result of two overlapping patterns corresponding to ZnPc nanocrystals with 0 0 1 and 0 0 −1 contact planes on the PC substrate. The unit cell parameters of α ZnPc are extracted from electron diffraction, HR-TEM images of ZnPc stacks and the X-ray diffraction measurements: $a$ = 1.23 nm, $b$ = 0.38 nm, $c$ = 1.28 nm and α = $\beta$ = 90° (±1°) and $\gamma$ = 96°. As seen in Table 1, these unit cell parameters are very close to those proposed for α-CuPc and α-CoPc, suggesting that the α forms of CuPc, CoPc

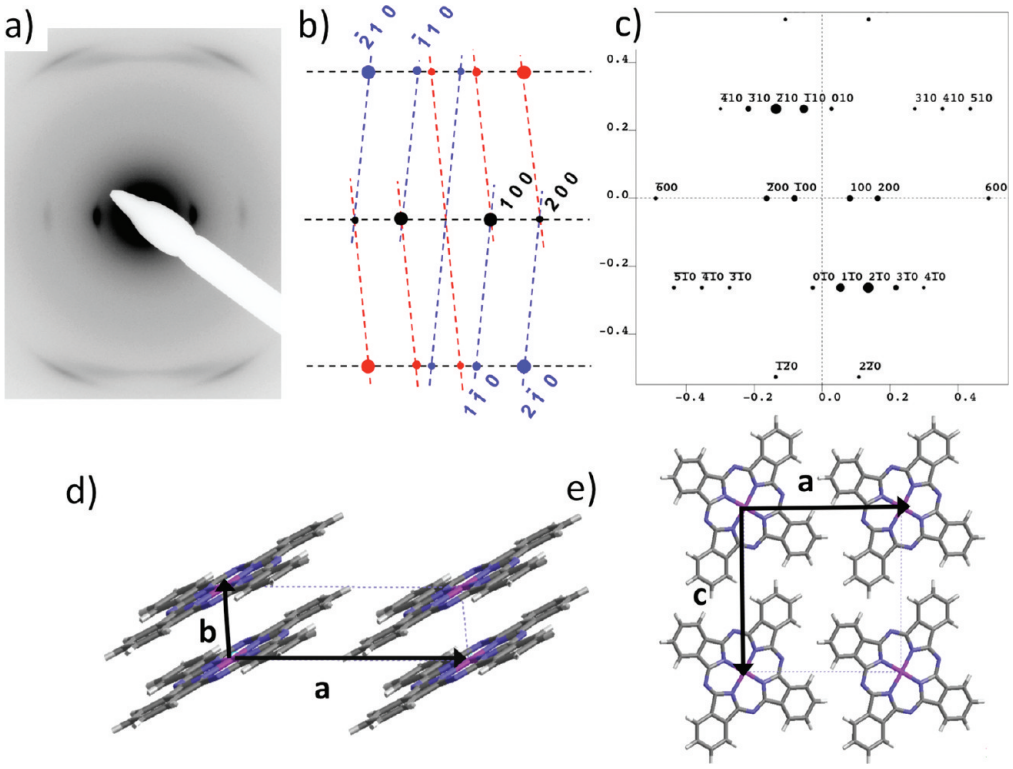


**Figure 11.** (a) Experimental ED pattern of α ZnPc film ($T_s$ = 115 °C) on PC substrate, (b) rationale of the ED pattern, (c) calculated ED pattern for the refined α structure. (d and e) Structural models of α-ZnPc viewed in projection along the **c** and **b** axes.

**Table 1. Unit Cell Parameters of Different α-Form Phthalocyanines**

| phthalocyanine/unit cell parameters | *a* (nm) | *b* (nm) | *c* (nm) | α (deg) | *β* (deg) | *γ* (deg) | ref no. |
|---|---|---|---|---|---|---|---|
| CuPc[a] | 1.20 | 0.381 | 1.29 | 91.0 | 90.1 | 95.6 | 24 |
| CoPc[b] | 1.209 | 0.375 | 1.280 | 88.96 | 90.97 | 95.09 | 22 |
| ZnPc[a] | 1.23 | 0.38 | 1.28 | - | - | 96 | this work |

[a] Prepared by high vacuum sublimation and. [b] Prepared by precipitation in water of a sulfuric acid solution of CoPc.

and ZnPc are isomorphous.[21−23] A structural model of α ZnPc was accordingly constructed using the Cerius2 program. Hoshino's models II of CuPc was used as a starting point, using the unit cell parameters given above and replacing the Cu atom by a Zn atom. The energy of the structure was minimized and the final structure is illustrated in Figure 11, parts d and e.[41] The calculated ED pattern for a crystal with (0 0 1) contact plane is shown in Figure 11c. Because of the tilt of the molecules in the columns, the calculated ED pattern is asymmetric with respect to the meridian. It accounts for the higher intensity of the (−2 1 0) reflection over (−1 1 0). Discrepancies in the relative intensity of 1 0 0 over 2 1 0 reflections may be related to the fact that the experimental patterns have been recorded in the presence of the PC substrate causing some unwanted electron scattering. The symmetry of the reflection's intensities with respect to the meridian in the experimental pattern results from the coexistence of ZnPc crystals with (0 0 1) and (0 0 −1) contact planes. As pointed by Kobayashi and co-workers for GeOPc, the coexistence of two contact planes implies the presence of specific fault planes at the interface between two nanocrystals.[42] In the case of α-ZnPc, a close packing of the molecules at the interface between two domains with (0 0 1) and (0 0 −1) contact planes can be obtained by introducing a relative displacement of the two lattices by a vector 1/2*c* (see Figure S1 of the Supporting Information).

Pure films of the *β*-form of ZnPc could not be obtained on the PC substrates even for $T_s$ = 200 °C. Accordingly, *β* form films were prepared in two steps: (i) evaporating a ZnPc films on PC at $T_s$ = 170 °C and (ii) floating the carbon-coated film on $CH_2Cl_2$. In this process, the PC substrate is dissolved in $CH_2Cl_2$ and the ZnPc film is converted to pure *β*-form by solvent annealing in the vapors of $CH_2Cl_2$. The *β* structure is identified by electron diffraction (Figure 12). The ED of the *β*-ZnPc films is compared with the calculated ED pattern using the *β* structure by Scheidt and Dow.[21] The experimental ED pattern can be interpreted as the overlap of two patterns corresponding to nearby [1 0 2] and [1 1 2] zone axes. As shown in Figure 12, both zone axes are nearly normal to the film surface and therefore can both contribute to the observed ED pattern. Accordingly, the structure of the *β* form of ZnPc films grown on PC substrates is isomorphous to the *β* structure of other metallophtalocyanines.[20,21]


dx.doi.org/10.1021/ma200350v |*Macromolecules* 2011, 44, 3817–3827

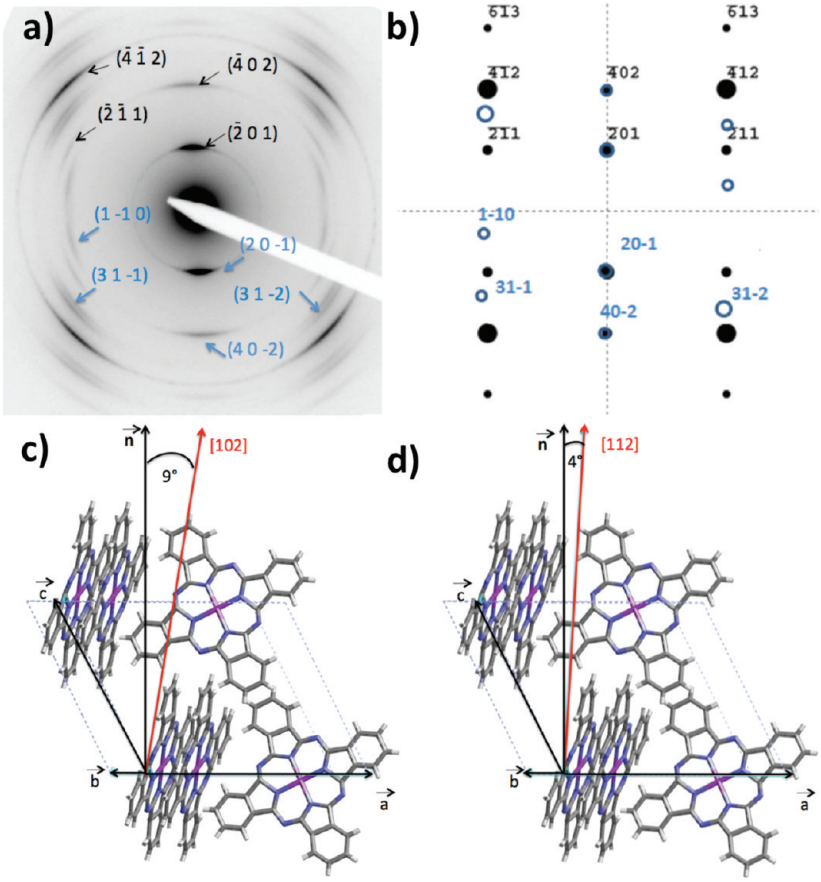


**Figure 12.** (a) ED pattern of a $\beta$-form ZnPc film (50 nm) on oriented PC substrate. (b) Calculated ED pattern showing contributions for [1 0 2] and [1 1 2] zone axes. (c and d) illustration of the [1 0 2] and [1 1 2] zone axes orientation with respect to the preferential (0 0 1) contact plane.

## IV. DISCUSSION

The growth mechanism of ZnPc on PC substrates and more specifically the development of in-plane orientation is schematically illustrated in Figure 13. It can be rationalized based on two characteristic length scales ; the typical mean diffusion path on the nanostructured PC substrate $\lambda_D$ and the lamellar period of the semicrystalline structure of PC, $\lambda_{PC}$. For $T_s \leq$ 33 °C, the nucleation density is such that impinging ZnPc molecules do not "see" the anisotropy of the nanocorrugated surface of the semi-crystalline PC substrate. The growth of the nanocrystals is essentially isotropic. As $T_s$ increases, the ZnPc molecules diffuse over a larger distance and when $\lambda_D > \lambda_{PC}$, they can probe the anisotropic topography of the surface of the PC substrate (amorphous interlamellar zones and oriented crystalline lamellae). ZnPc molecules apparently diffuse more readily in the direction parallel to the lamellae of PC and this mechanism is enhanced with increasing substrate temperature. This anisotropic diffusion enhances the growth of the nanocrystals so that the ZnPc molecules are stacked in a direction parallel to the PC lamellae i.e. $\mathbf{b}_{ZnPc}//\mathbf{a}_{Pc}$. However, this effect becomes operative only at larger $T_s$. Indeed, for $T_s$ = 60 °C, two dominant in-plane orientations of the ZnPc nanocrystals still coexist: $\mathbf{b}_{ZnPc}\| \mathbf{a}_{PC}$ and $\mathbf{b}_{ZnPc}\| \mathbf{c}_{PC}$. For $T_s$ = 100 °C, the population of nanocrystals with $\mathbf{b}_{ZnPc}\| \mathbf{a}_{PC}$ becomes dominant. This trend points to a competition between different in-plane orientation mechanisms of the ZnPc nanocrystals. It also suggests that the selection of a preferred in-plane orientation is favored by the increase of the substrate temperature i.e. the nanocrystal orientation mechanism must relie on thermally activated processes, e.g., anisotropic surface diffusion or coalescence and re-orientation of ZnPc nanodomains.

The results also indicate that the in-plane orientation of the ZnPc nanocrystals sets in as the film thickness increases above a certain minimum thickness close to 15 nm. For $t$ = 15 nm, only a fraction of the ZnPc nanocrystals orients parallel to the PC lamellae, whereas for $t$ = 50 nm the majority of ZnPc nanocrystals are oriented in this direction. HR-TEM images of the α-ZnPc films grown at $T_s$ = 100 °C (Figure 3) demonstrate that the elongated nanocrystals are formed by aggregation of smaller nanocrystalline domains as in the case of titanyl phthalocyanine on PTFE substrates.[38] This implies that the in-plane orientation is a "self-amplified" phenomenon; i.e., the in-plane orientation of the nanocrystals improves as the film thickness increases. In other words, the first oriented nanocrystals guide and enforce the selection of the in-plane growth direction of the surrounding nanocrystals that continue to grow. The oriented character of the substrate is responsible for (i) the anisotropic surface diffusion of ZnPc molecules and (ii) the nucleation of a fraction of oriented ZnPc nanocrystals.

In many instances, orientation of molecular materials was described in terms of epitaxy i.e. matching of unit cell parameters of the overlayer and the substrate.[43,44] For the dominant population of α nanocrystals, the orientation on the PC substrate is characterized by $[0\ 1\ 0]_{\alpha\text{-ZnPc}}\| [1\ 0\ 0]_{PC}$ and $(0\ 0\ 1)_{\alpha\text{-ZnPc}}\| (0\ 1\ 0)_{PC}$. The following epitaxial condition may

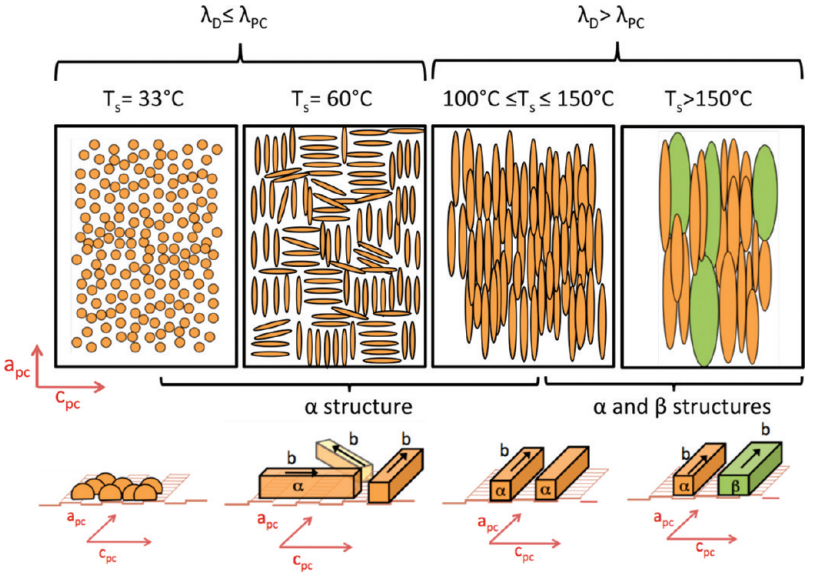


**Figure 13.** Rationale of the growth mechanism of ZnPc thin films on oriented and nanostructured PC substrates as a function of increasing substrate temperature.

apply: $3b_{\alpha-\mathrm{ZnPc}} \cong a_{\mathrm{PC}}$ (7%). For the $\beta$ phase, the relative orientation of ZnPc nanocrystals and PC substrate is such that: $[0\ 1\ 0]_{\beta\text{-ZnPc}} \| [1\ 0\ 0]_{\mathrm{PC}}$ and $(0\ 0\ 1)_{\beta\text{-ZnPc}} \| (0\ 1\ 0)_{\mathrm{PC}}$. Considering the unit cell parameters of the $\beta$-form ZnPc overlayer and the PC substrate, no clear epitaxial orientation can be found. Given the coexistence of α and $\beta$ phases in a large range of $T_s$, the $\beta$ form may also be oriented by an underlying layer of oriented α form and not necessarily by the PC substrate. Nevertheless, the interface structure between the PC substrate and the two ZnPc polymorphs suggest that the preorientation of the ZnPc nuclei on the substrate does not necessarily involve an epitaxial mechanism as pointed out in our previous study for substituted phthalocyanines on PC substrates.[32]

The present results show that the onset of the $\beta$ form growth for $T_s$ = 100−115 °C coincides with a steep variation of both width and length of the nanocrystals. This observation suggests that the emergence of the $\beta$ form could be determined by size effects as proposed originally by Iwatsu.[29] Following a similar approach, Drummy et al. have determined the critical thickness in pentacene films for which the triclinic phase is favored over the orthorhombic phase when the film thickness exceeds a threshold value of approximately 30 nm.[30] Herein the $\beta$ form of ZnPc is formed in the films when the size of the nanocrystals exceeds some threshold dimensions by changing the substrate temperature. The competition between the formation of the α and $\beta$ polymorphs has been modeled by estimating the total free energy of the nanocrystals using three contributions: (i) the volumic free energy, (ii) the surface energy of the $h\ k\ l$ facets $\gamma^{i}_{hkl}$ and (iii) the interfacial energy $\gamma^{i}_{001}$ of the nanocrystal with the substrate for the phase labeled i (i = α or $\beta$) (for both the α and $\beta$ phases, the nanocrystals have a preferential (0 0 1) contact plane with the PC substrate). The model described hereafter gives the critical dimensions of the ZnPc crystal for which the phase change occurs (for a fixed film thickness). In the following, we assume a rhombic shape of the ZnPc nanocrystal of phase i (i = α or $\beta$) of dimensions $l_a$, $l_b$, and $l_c$ along the crystallographic directions $a$, $b$, and $c$ respectively with a preferential (0 0 1) contact plane on the substrate. The energy $E^{i}$ of the nanocrystal of phase i can accordingly be written as

$$E^{i} = l_a l_b l_c E^{i}_{\mathrm{bulk}} + l_a l_b \gamma^{i}_{s} + l_a l_b \gamma^{i}_{001} + 2 l_c l_b \gamma^{i}_{100} \qquad (1)$$

where $\gamma^{i}_{s}$ is the interfacial energy between the (0 0 1) face of the nanocrystal and the PC substrate. The critical dimension of the nanocrystal is reached when $E^{\alpha} = E^{\beta}$. It turns out that the critical dimension of the nanocrystals is independent of the length of the nanocrystals $l_b$. For a thin film of thickness $t$, assuming that $l_c = t$, the phase transformation occurs when the width of the nanocrystals reaches a critical value $w^* = l_a$ given by the following expression:

$$w^* = \frac{2 l_c (\gamma^{\beta}_{100} - \gamma^{\alpha}_{100})}{l_c (E^{\alpha}_{\mathrm{bulk}} - E^{\beta}_{\mathrm{bulk}}) + (\gamma^{\alpha}_{s} - \gamma^{\beta}_{s}) + (\gamma^{\alpha}_{001} - \gamma^{\beta}_{001})} \qquad (2)$$

To estimate $w^*$, we have calculated the surface and bulk free energies of the α and $\beta$ structures, using the structural model of the α form determined herein. The bulk free energies calculated for the α and $\beta$ forms amount to −274.6 kJ/mol and −285.0 kJ/mol respectively (using only van der Waals interactions and the universal force field[41]). These values are close to those obtained by Iwatsu alltough slightly overestimated.[29] Surface energies of the (1 0 0) and (0 0 1) facets of the α and $\beta$ polymorphs have been evaluated by simulating a crystal cleavage. The surface energy of the (0 0 1) and (1 0 0) facets can be approximated by calculating the energy of interaction between two crystal slabs along the corresponding cleavage planes using the Cerius2 (version 4.6) program and dividing it by two times the surface of the slab. Only van der Waals interactions have been taken into account. A first verification was made to follow the dependence of the calculated surface energy on the thickness of the slab normal to the cleavage plane using 1, 2, or 3 ZnPc layers. It was found that one layer of ZnPc molecules was sufficient to estimate $\gamma^{i}_{hkl}$ (i = α,$\beta$). A similar approach was followed for the dimensions of the slab in the cleavage plane. Absence of boundary effects are observed when

the dimensions of the slab in the cleavage plane are 10 unit cells along the stacking direction ($b$ axis for both polymorphs) and 5 molecular repeat units along the perpendicular direction ($a$ or $c$ axis). As an example, for the (0 0 1) cleavage plane of the α structure, the size of slab was $5a \times 10b$ whereas for the (1 0 0) plane it was $5c \times 10b$. For the α polymorph, we obtained $\gamma^{\alpha}_{100}$ = 82 mJ/m$^2$ and $\gamma^{\alpha}_{001}$ = 60 mJ/m$^2$ . For the $\beta$ structure: $\gamma^{\beta}_{100}$ = 105 mJ/m$^2$ and $\gamma^{\beta}_{001}$ = 71 mJ/m$^2$.

An estimation for the interfacial term $(\gamma^{\beta}_{s} - \gamma^{\alpha}_{s})$ was obtained by using the equation $\gamma^{i}_{s} = ((\gamma_{PC})^{1/2} - (\gamma^{i}_{001})^{1/2})^2$ where the index i refers to the α and $\beta$ structures.[45] Using the surface free energy of PC, $\gamma_{PC}$ = 40 mJ/m$^2$[46] we could estimate the interfacial term to ≈2 mJ/m$^2$. Inserting now the different numerical values into eq 1, we derive a critical width $w^*$ of the ZnPc nanocrystals in the range 200−300 nm. The calculated value of w is larger but close to the experimental value in the range 100−150 nm (see Figure 5). However, it has to be stressed that the present calculations can only give a rough estimate of the critical dimensions of the nanocrystals as the exact calculations of surface free energies would imply to estimate the entropic part related to the relaxation of the surface structure upon cleavage. In addition, as noted by Drummy et al.,[30] the values of the calculated surface energies are often overrated and depend strongly on the chosen force field. Nevertheless, the present analysis supports previous assumptions by Iwatsu et al. that the phase changes in ZnPc thin films can be induced by competing bulk and surface free energies of two polymorphic forms.[29,30]

## V. CONCLUSION

This work has uncovered several important aspects concerning the growth of ZnPc nanocrystals on oriented and nanostructured PC substrates. First, the oriented crystalline lamellae of the PC substrate show a preferential ($a$, $c$) surface of the crystalline and oriented lamellae. Second, the orientation mechanism of ZnPc is by essence "auto-catalytic", i.e., the preferred in-plane orientation of the ZnPc nanocrystals parallel to the PC lamellae sets in progressively and amplifies during the growth of the nanocrystals. Comparison of AFM needle morphology and HR-TEM investigations of the ZnPc films indicate that the oriented ZnPc needles are polycrystalline, i.e., formed by coalescence of crystalline nanodomains. Third, the evolution of the polymorphism with substrate temperature $T_s$ has been carefully analyzed and two temperature ranges have been identified: for $T_s \leq 115$ °C, the films grow exclusively in the α form and the nanocrystals are oriented such that $(0\ 0\ 1)_{\alpha\text{-ZnPc}} \| (0\ 1\ 0)_{PC}$ and $[0\ 1\ 0]_{\alpha\text{-ZnPc}} \| [1\ 0\ 0]_{PC}$. The crystal structure of the α form is found to be isomorphous to that reported recently for CuPc and CoPc. For 115 °C $\leq T_s \leq$ 200 °C, the films are polymorphic with coexisting α and $\beta$ domains whose columns still orient parallel to the crystalline lamellae of the PC substrate. Even for $T_s$ = 200 °C, the films do not consist of pure $\beta$ form. Finally, the onset of the α → $\beta$ phase transformation coincides with a steep change in the nanocrystal dimensions around $T_s$ = 100−115 °C. The structural change sets in when the width of the needle-shaped crystals exceeds a threshhold value of ∼100 nm. This value is tentatively explained in terms of the surface and bulk energy contributions of the α and $\beta$ structures.

## ■ ASSOCIATED CONTENT

**Supporting Information.** Schematic illustration of the possible molecular packing between two α-ZnPc aggregates. This material is available free of charge via the Internet at http://pubs.acs.org.

## ■ AUTHOR INFORMATION

**Corresponding Author**
*E-mail: brinkman@ics.u-strasbg.fr.

## ■ ACKNOWLEDGMENT

Christophe Contal is acknowledged for his valuable help in AFM. Dr. Bernard Lotz is acknowledged for constructive and helpful advices. Prof. Christine Petit (ECPM, Strasbourg) is acknowledged for her kind assistance in the X-ray diffraction measurements.

## ■ REFERENCES

(1) Bart, J. V.; Costantini, G.; Kern, K. *Nature* **2005**, *437*, 671.
(2) Bowden, N.; Brittain, S.; Evans, A. G.; Hutchinson, J. W.; Whitesides, G. M. *Nature* **1998**, *393*, 146.
(3) Fruchart, O.; Klaua, M.; Barthel, J.; Kirschner, J. *Phys. Rev. Lett.* **1999**, *83*, 2769.
(4) Meyer zu Heringdorf, F. J.; Reuter, M. C.; Tromp, R. M. *Nature* **2001**, *412*, 517.
(5) Vonau, F.; Suhr, D.; Aubel, D.; Bouteiller, L.; Reiter, G.; Simon, L. *Phys. Rev. Lett.* **2005**, *94*, 066103.
(6) Barrena, E.; de Oteyza, D. G.; Sellner, S.; Dosch, H.; Osso, J. O.; Struth, B. *Phys. Rev. Lett.* **2006**, *97*, 76102.
(7) Umbach, E.; Sokolowski, M.; Fink, R. *Appl. Phys. A: Mater. Sci. Process.* **1996**, *63*, 565.
(8) Yang, J.; Yan, D. *Chem. Soc. Rev.* **2009**, *38*, 2634.
(9) Karl, N. *Synth. Met.* **2002**, *133*, 649.
(10) Virkar, A. A.; Mannsfeld, S.; Bao, Z.; Stingelin, N. *Adv. Mater.* **2010**, *22*, 3857.
(11) Leznoff, C. C.; Lever, A. B. P. *Phthalocyanines Properties and Applications*, VCH Publishers: Weinheim, Germany, 1989, 1993, 1994, and 1996; Vols 1, 2, 3, and 4.
(12) Brabec, C . J.; Sariciftci, N. S.; Hummelen, J. C. *Adv. Funct. Mat.* **2001**, *11*, 15.
(13) Bruder, I.; Schöneboom, J.; Dinnebier, R.; Ojala, A.; Schaäfer, S.; Sens, R.; Erk, P.; Weiss, J. *Org. Elect.* **2010**, *11*, 377.
(14) Heim, C.; Mankel, E.; Mayer, T.; Jaegermann, W. *Sol. Energy Mater. Sol. Cells* **2010**, *94*, 662.
(15) (a) Rostalski, J.; Meissner, D. *Sol. Energy Mater. Sol. Cells* **2000**, *61*, 87. (B) Rostalski, J.; Meissner, D. *Sol. Energy Mater. Sol. Cells* **2000**, *63*, 37. (c) Tsuzuki, T.; Shirota, Y.; Rostalski, J.; Meissner, D. *Sol. Energy Mater. Sol. Cells* **2000**, *61*, 1.
(16) Dimitrakopoulos, C. D.; Brown, A. R.; Pomp, A. *J. Appl. Phys.* **1996**, *80*, 2501.
(17) Pfattner, R.; Mas-Torrent, M.; Bilotti, I.; Brillante, A.; Milita, S.; Liscio, F.; Biscarini, F.; Marszalek, T.; Ulanski, J.; Nosal, A.; Gazicki-Lipman, M.; Leufgen, M.; Schmidt, G.; Molenkamp, L. W.; Laukhin, V.; Veciana, J.; Rovira, C. *Adv. Funct. Mater.* **2010**, *22*, 4198.
(18) Kobayashi, T.; Fujiyoshi, Y.; Iwatsu, F.; Uyeda, N. *Acta Crystallogr. A* **1981**, *37*, 692.
(19) Brown, C. J. *J. Chem. Soc.* **1968**, 2488.
(20) Kirner, J. F.; Dow, W.; Scheidt, W. R. *Inorg. Chem.* **1976**, *15*, 1685.
(21) Scheidt, W. R.; Dow, W. *J. Am. Chem. Soc.* **1977**, *99*, 1101.
(22) Ballirano, P.; Caminiti, R.; Ercolani, C.; Maras, A.; Orrù, M. A. *J. Am. Chem. Soc.* **1998**, *120*, 12798.

(23) Erk, P.; Hengelsberg, H.; Haddow, M. F.; van Gelder, R. *Cryst. Eng. Comm.* **2004**, *6*, 474.
(24) Hoshino, A.; Takenada, Y.; Miyaji, H. *Acta. Crystallogr. B* **2003**, *B59*, 393.
(25) Hassan, A. K.; Gould, R. D. *Phys. Status Solidi A* **1992**, *132*, 91.
(26) Brinkmann, M.; Chaumont, C.; Wachtel, H.; André, J. -J. *Thin Solid Films* **1996**, *283*, 97.
(27) Iwatsu, F.; Kobayashi, T.; Uyeda, N. *J. Phys. Chem.* **1980**, *84*, 3223.
(28) Brinkmann, M.; Wittmann, J.-C.; Chaumont, C.; André, J.-J. *Thin Solid Films* **1997**, *283*, 97.
(29) Iwatsu, F. *J. Phys. Chem.* **1998**, *92*, 1678.
(30) Drummy, L. F.; Martin, D. C. *Adv. Mater.* **2005**, *17*, 903.
(31) Brinkmann, M.; Pratontep, S.; Chaumont, C.; Wittmann, J.-C. *Macromolecules* **2007**, *40*, 9420.
(32) Vergnat, C.; Uttiya, S.; Pratontep, S.; Kerdcharoen, T.; Legrand, J.-F.; Brinkmann, M. *Synth. Met.* **2011**, *161*, 251.
(33) Pratontep, S.; Brinkmann, M.; Nüesch, F.; Zuppiroli, L. *Phys. Rev. B* **2004**, *69*, 165201S.
(34) Pratontep, F.; Nüesch, L.; Zuppiroli; Brinkmann, M. *Phys. Rev. B* **2005**, *72*, 85211.
(35) Bonart, R. *Makromol. Chem.* **1966**, *92*, 149.
(36) Vergnat, C. Ph.D. thesis, University of Strasbourg, Strasbourg, France.
(37) Toney, M. F.; Russell, T. P.; Logan, J. A.; Kikuchi, H.; Sands, J. M.; Kumar, S. K. *Nature* **1995**, *374*, 709.
(38) Brinkmann, M.; Wittmann, J.-C.; Barthel, M.; Hanack, M.; Chaumont, C. *Chem. Mater.* **2002**, *14*, 904.
(39) Brinkmann, M.; Graff, S.; Straupé, C.; Wittmann, J.-C.; Chaumont, C.; Nüesch, F.; Aziz, A.; Schaer, M.; Zuppiroli, L. *J. Phys. Chem. B* **2003**, *107*, 10531.
(40) Plank, H.; Resel, R.; Purger, S.; Keckes, J.; Thierry, A.; Lotz, B.; Andreev, A.; Sariciftci, N. S.; Sitter, H. *Phys. Rev. B* **2001**, *64*, 235423.
(41) Castonguay, L. A.; Rappe, A. K. *J. Am. Chem. Soc.* **1992**, *114*, 5832.
(42) Kobayashi, T. In *Organic Crystals I: characterization*, Karl, N.; Ed.; Springer Verlag: Berlin, 1991; p 46.
(43) Ward, M. D. *Chem. Rev.* **2001**, *101*, 1697.
(44) Jiang, S.; Qian, H.; Liu, W.; Wang, C.; Wang, Z.; Yan, S.; Zhu, D. *Macromolecules* **2009**, *42*, 9321.
(45) Israelachvili, J. N. *Intermolecular and surface forces*; Academic Press: San Diego, CA, 1985; p 115.
(46) Kitova, S.; Minchev, M.; Danev, G. *J. Optoelectron. Adv. Mater.* **2005**, *7*, 2607.